Available online at www.sciencedirect.com
SCIENCE DIRECT®
International Journal of Heat and Mass Transfer 49 (2006) 2180–2189
International Journal of HEAT and MASS TRANSFER
www.elsevier.com/locate/ijhmt

Prediction of protective banks in high temperature smelting furnaces by inverse heat transfer

Ouafa Tadrari, Marcel Lacroix *

Department of Mechanical Engineering, University of Sherbrooke, Sherbrooke, Canada J1K 2R1

Received 8 April 2005; received in revised form 23 November 2005
Available online 28 February 2006

Abstract

An inverse phase change heat transfer method has been developed for predicting the time evolution of banks covering the surface of refractory brick walls inside high temperature smelting furnaces. The presence of these banks is indispensable as they serve as a protective barrier against the highly corrosive slag, thereby maintaining the structural integrity of the furnace and prolonging its active life. The numerical model rests on the conjugate gradient solution method with the adjoint equation. It predicts banks thickness and motion relying on the thermal conditions prevailing outside the furnace and temperature measurements taken at one location inside the brick wall. Simulations are carried out to examine the effect of different parameters on the predictive capabilities of the method. Results reveal that the method remains accurate in spite of the fact that the temperature measurements inside the wall are noisy and are taken at depth of few centimetres only. An example showing how the present inverse method can be used to warn on the imminent loss of the protective bank during the operation of a smelting furnace is then provided.

Keywords: Inverse heat transfer; Solid liquid phase change; Furnace

1. Introduction

Electric arc furnaces (EAFs) are used for material processing that requires high powers and temperatures. Their main applications are the smelting of materials such as copper, nickel calcine, steel, pre-reduced iron ore and the melting/recycling of scrap metals from the automobile and metallurgical manufacturing industries [1]. As an example, a cross view of a typical electric arc smelting furnace is depicted in Fig. 1. High voltage electrodes (only one electrode is shown here) discharge their electric load in a bath of electrically conducting slag. The current is carried between the electrode tips in the slag to generate the heat (Joule effect) required for the smelting process. Continuous loading of grained ore is achieved via openings in the vault. The smelting reaction takes place in the slag layer and heat is transferred to the metal layer through the slag/metal interface and via metal droplets that fall at the bottom of the bath. Tapping of slag and metal is carried out at regular time intervals through holes perforated in the lateral walls. The furnace experiences heat losses from the surface of the slag to the freeboard gas and to the water cooled vault and through the refractory brick walls. Few thermocouples are usually embedded in the refractory brick walls to monitor their temperature and, as it will be seen in the next section, to provide some information on the thermal conditions prevailing inside the furnace.

A fascinating melting/solidification problem that arises in this type of high power smelting furnace is the formation of solid layers, called banks, on the inside surface of the refractory brick walls (Fig. 1). The presence of these banks is indispensable as they serve as a protective barrier against the highly corrosive slag, thereby maintaining the integrity of the furnace and prolonging its active life. On the other hand, too thick a bank is detrimental to the furnace throughput as the volume available for smelting is reduced.

* Corresponding author. Tel.: +1 819 821 8000; fax: +1 819 821 7163.
E-mail address: Marcel.lacroix@usherbrooke.ca (M. Lacroix).

0017-9310/$ - see front matter © 2006 Elsevier Ltd. All rights reserved.
doi:10.1016/j.ijheatmasstransfer.2005.11.023

Nomenclature

C	heat capacity (J/kg K)
D	studied configuration thickness (m)
d	wall thickness (m)
$d(t)$	direction of descent [Eq. (5b)]
e_1, e_2	estimation errors [Eqs. (20) and (21)]
$f(x, t)$	liquid fraction
h	average heat transfer coefficient (W/m^2 K)
k	thermal conductivity (W/m K)
L	latent heat (J/kg)
$q''(t)$	heat flux (W/m^2)
R''_{cont}	thermal contact resistance (m^2 K/W)
$E_b(t)$	bank thickness (m)
$S[q''(t)]$	objective functional [Eq. (4)]
t	time (s)
$T(x, t)$	temperature defined by problem, Eqs. (1)
T_∞	surrounding temperature (K)
T_l	liquidus temperature (K)
$T_m(t)$	measured temperature (K)
T_{ref}	reference temperature (K)
T_s	solidus temperature (K)
x	Cartesian spatial coordinate (m)
x_m	measurement position (m)

Greek symbols

$\delta(\cdot)$	Dirac delta function
$\nabla S[q''(t)]$	gradient direction [Eq. (16)]
β	search step size [Eq. (10)]
γ	coefficient [Eq. (5c)]
Δ	small variation
δH	enthalpy (J/m^3)
$\Delta T(x, t)$	sensitivity function defined by problem, Eqs. (9)
ε	real number
$\lambda(x, t)$	Lagrange multiplier defined by problem, Eqs. (14)
ρ	density (kg/m^3)
σ	standard deviation of measurement error
ω	Gaussian distributed random number

Subscripts

0	initial value
1	value in the brick wall
2	value in the slag
f	final value
l	liquid phase
s	solid phase

Superscript

k	iteration number

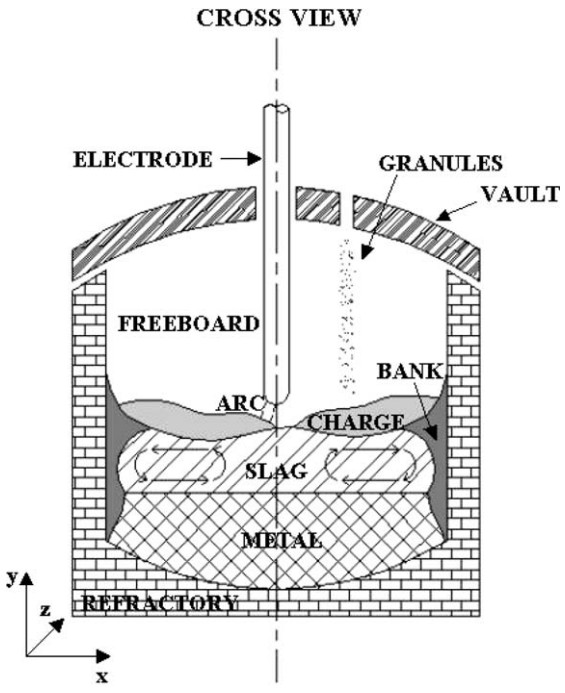

Fig. 1. Cross view of a typical smelting furnace.

Keeping banks of optimal size is therefore crucial for the safe and profitable operation of smelting furnaces. Unfortunately, due to the hostile conditions that prevail in the bath, probing their shape and their motion is a difficult task. An alternative is to predict their behaviour with an inverse heat transfer method. This is precisely the objective of the present study.

In spite of the fact that investigations have been conducted to predict the heat transfer and flow circulation in pools of EAFs [2–4], none however have examined the problem of banks formation. The transient formation of banks is a complex problem that depends on the energy transfer from the electrodes to the slag layer (the transferred arc), on the heat transfer phenomena prevailing inside the pool and on the way the furnace is designed and operated. Direct solution of the heat transfer and flow circulation in the pool for predicting the banks shape and motion is feasible with modern CFD tools but this approach is too complex and time consuming to be implemented on line in a control system. Predicting banks formation with an inverse phase change method appears to be a very promising method.

2. Problem statement and mathematical model

Fig. 2 illustrates the one-dimensional geometry analysed in the present problem. A thermocouple is embedded at a depth x_m inside the lateral brick wall for recording the

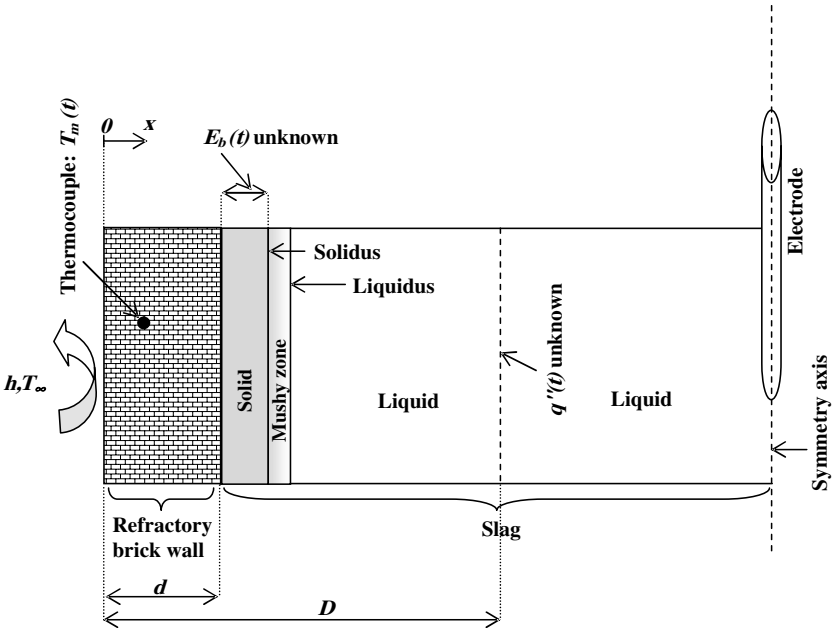

Fig. 2. Schematic of the inverse heat transfer problem.

transient temperature $T_m(t)$. The thermal conditions prevailing outside the furnace, i.e., T_∞ and h, are also known. The inverse problem then consists of finding the heat flux $q''(t)$, i.e., the right boundary condition at $x = D$, that yields the measured temperature $T_m(t)$. Once this is achieved, the bank thickness $E_b(t)$ is easily predicted with a direct phase change heat transfer method [5]. The time function $E_b(t)$ is calculated as the distance between the inside surface of the refractory brick wall and the solidus position.

Inverse heat conduction problems with phase change have received, over the last two decades, increasing research attention in the open literature [6–13]. These investigations focused chiefly on four types of inverse phase change problems: (1) the melting problem of calculating the moving front position from temperature measurement in the solid phase [8–12]; (2) the solidification problem of calculating the front position and boundary fluxes from temperature measurements in the solid and liquid phases [6]; (3) the design problem of calculating the required cooling boundary conditions that achieve desired freezing front motion and interface fluxes [7] and (4), the problem of thermal contact resistance estimation during the solidification process [13]. These problems were investigated with applications to melting, welding and casting. None of the afore mentioned studies have examined however the problem of banks formation inside high power smelters.

In the present paper, the inverse problem of banks formation is examined by employing the conjugate gradient solution method with the adjoint equation [13,14]. The method is adapted to nonlinear heat conduction with non-isothermal solid/liquid phase change.

3. The direct problem

The mathematical model rests on the following assumptions:

1. The flow circulation in the slag layer is highly turbulent and multiphase (solid/liquid/gas). Flow circulation is caused by a combination of factors, namely, the transfer of jet momentum at the bath surface, the natural convection resulting from thermal gradients in the system, the gas bubble driven circulation and the electromagnetic (Lorentz) forces induced due to the passage of electric current. Taking into account the combined effects of theses forces is beyond the scope and the objectives of the present study. One of the consequences of the strong flow circulation is, however, that the temperature of the liquid phase is uniform. As a result, it is assumed that heat transfer in the liquid phase is conduction dominated and the effect of the vigorous flow circulation is accounted for by means of an empirically adjusted thermal conductivity $k_{l,\mathrm{eff}} \gg k_l$ in the liquid phase. In spite of its boldness and simplicity, this approach was successfully used in the past for predicting the overall thermal behaviour of melting furnaces [15].
2. The temperature gradients across the wall (x direction) are much larger than the temperature gradients in the vertical direction so that a one-dimensional analysis can be applied.
3. The phase change problem is nonisothermal.
4. The thermal contact resistance between the refractory brick wall and the slag bank is neglected.
5. The slag thermal properties are temperature dependent.

With the foregoing assumptions, the governing equations and boundary conditions may be stated as

For the brick wall:

$$\rho_1 C_1 \frac{\partial T_1}{\partial t} = k_1 \frac{\partial^2 T_1}{\partial x^2}; \quad 0 < x < d \text{ and } 0 < t \leqslant t_f \tag{1a}$$

$$k_1 \frac{\partial T_1}{\partial x} = h(T_1 - T_\infty); \quad x = 0 \text{ and } 0 < t \leqslant t_f \tag{1b}$$

$$T_1 = T_{01}; \quad 0 < x < d \text{ and } t = 0 \tag{1c}$$

For the slag bath:

$$\rho_2 C_2(T_2) \frac{\partial T_2}{\partial t} = \frac{\partial}{\partial x}\left(k_2(T_2)\frac{\partial T_2}{\partial x}\right) - \delta H \frac{\partial f}{\partial t}; \quad d < x < D \text{ and } 0 < t \leqslant t_f \tag{1d}$$

$$k_2(T_2)\frac{\partial T_2}{\partial x} = q''(t); \quad x = D \text{ and } 0 < t \leqslant t_f \tag{1e}$$

$$T_2 = T_{02}; \quad d < x < D \text{ and } t = 0 \tag{1f}$$

At the wall/slag interface:

$$k_1 \frac{\partial T_1}{\partial x} = k_2(T_2)\frac{\partial T_2}{\partial x}; \quad x = d \text{ and } 0 < t \leqslant t_f \tag{1g}$$

$$T_1 = T_2; \quad x = d \text{ and } 0 < t \leqslant t_f \tag{1h}$$

The second term on the right-hand side of Eq. (1d) accounts for the solid/liquid phase change. The enthalpy δH is defined as $\delta H = \rho_2(C_{2l} - C_{2s})(T_2 - T_{ref}) + \rho_2 L$. The liquid fraction $f(x, t)$ varies linearly between the solidus T_s and the liquidus T_l in the following manner:

$$f = F(T_2) = \begin{cases} 0; & T_2 \leqslant T_s \\ \frac{T_2 - T_s}{T_l - T_s}; & T_s < T_2 < T_l \\ 1; & T_2 \geqslant T_l \end{cases} \tag{2}$$

The direct problem given by the set of Eqs. (1) is concerned with the determination of the temperature fields $T_1(x, t)$ and $T_2(x, t)$ for the brick wall and the slag bath, respectively, when the boundary heat flux $q''(t)$ at $x = D$ is known.

4. The inverse problem

For the inverse problem, the heat flux $q''(t)$ at $x = D$ is unknown. It may be estimated however by using the transient reading $T_m(t)$ of the thermocouple located inside the brick wall at position $x = x_m$. It is assumed here that no information is available regarding the functional form of the unknown boundary heat flux, except that it belongs to the space of square functions in $(0, t_f)$, i.e.,

$$\int_0^{t_f} [q''(t)]^2 \mathrm{d}t < \infty \tag{3}$$

where t_f is the time duration of the experiment. The solution of the inverse problem is then sought by minimizing the functional

$$S[q''(t)] = \int_0^{t_f} [T_m(t) - T_1(x_m, t; q''(t))]^2 \mathrm{d}t \tag{4}$$

where $T_m(t)$ is the measured temperature at the sensor location x_m and $T_1(x_m, t; q''(t))$ is the estimated temperature at the same location. The estimated temperature $T_1(x_m, t; q''(t))$ is obtained from the solution of the direct problem given by the set of Eqs. (1) using an estimated heat flux $q''(t)$. Eq. (4) is solved by employing the conjugate gradient method with the adjoint problem, as described next.

5. The conjugate gradient method

The iterative procedure for the conjugate gradient method, as applied to the estimation of the unknown heat flux $q''(t)$, is given by [14]:

$$q''^{k+1}(t) = q''^{k}(t) - \beta^k d^k(t) \tag{5a}$$

where the superscript k denotes the iteration number. The direction of descent $d^k(t)$ is approximated from the previous direction of descent $d^{k-1}(t)$:

$$d^k(t) = \nabla S[q''^k(t)] + \gamma^k d^{k-1}(t) \tag{5b}$$

The conjugation coefficient is defined here by the Polak-Ribiere expression:

$$\gamma^k = \frac{\int_0^{t_f} \{\nabla S[q''^k(t)] - \nabla S[q''^{k-1}(t)]\}\nabla S[q''^k(t)]\mathrm{d}t}{\int_0^{t_f} \{\nabla S[q''^{k-1}(t)]\}^2 \mathrm{d}t} \quad \text{for } k = 1, 2, 3, \ldots \tag{5c}$$

with $\gamma^0 = 0$. In order to implement the iterative procedure exemplified by Eqs. (5), one needs to develop expressions for the search step size β^k and for the gradient direction $\nabla S[q''^k(t)]$, by making use of two auxiliary problems, known as the sensitivity problem and the adjoint problem, respectively.

6. The sensitivity problem and the search step size

The sensitivity functions $\Delta T_1(x, t)$ and $\Delta T_2(x, t)$ for of the perturbation of the unknown function are defined as the directional derivatives of the temperatures $T_1(x, t)$ and $T_2(x, t)$, respectively. When the heat flux $q''(t)$ is perturbed by an amount $\varepsilon \Delta q''(t)$, the temperatures $T_1(x, t)$ and $T_2(x,t)$ experience variations $\varepsilon \Delta T_1(x, t)$ and $\varepsilon \Delta T_2(x, t)$, respectively, i.e.,

$$T_{1\varepsilon}(x, t) = T_1(x, t) + \varepsilon \Delta T_1(x, t) \quad \text{and}$$
$$T_{2\varepsilon}(x, t) = T_2(x, t) + \varepsilon \Delta T_2(x, t) \tag{6a}$$

ε is a real number and, when used as a subscript, it refers to a perturbed variable. Due to the nonlinear character of the heat transfer problem in the slag, the perturbation in the temperature $T_2(x, t)$ causes variations on the temperature-dependent properties of the slag, as well as on the liquid fraction given by Eq. (2). The resulting perturbed quantities are linearized as

$$k_{2\varepsilon}(T_{2\varepsilon}) = k_2(T_2 + \varepsilon\Delta T_2) \approx k_2(T_2) + \left(\frac{\mathrm{d}k_2}{\mathrm{d}T_2}\right)\varepsilon\Delta T_2 \tag{6b}$$

$$C_{2\varepsilon}(T_{2\varepsilon}) = C_2(T_2 + \varepsilon\Delta T_2) \approx C_2(T_2) + \left(\frac{\mathrm{d}C_2}{\mathrm{d}T_2}\right)\varepsilon\Delta T_2 \tag{6c}$$

$$F_{\varepsilon}(T_{2\varepsilon}) = F(T_2 + \varepsilon\Delta T_2) \approx F(T_2) + \left(\frac{\mathrm{d}F}{\mathrm{d}T_2}\right)\varepsilon\Delta T_2 \tag{6d}$$

The perturbed form of the direct problem (Eqs. (1)) is then written as

For the brick wall:

$$\rho_1 C_1 \frac{\partial T_{1\varepsilon}}{\partial t} = k_1 \frac{\partial^2 T_{1\varepsilon}}{\partial x^2}; \quad 0 < x < d \text{ and } 0 < t \leqslant t_{\mathrm{f}} \tag{7a}$$

$$k_1 \frac{\partial T_{1\varepsilon}}{\partial x} = h(T_{1\varepsilon} - T_{\infty}); \quad x = 0 \text{ and } 0 < t \leqslant t_{\mathrm{f}} \tag{7b}$$

$$T_{1\varepsilon} = T_{01}; \quad 0 < x < d \text{ and } t = 0 \tag{7c}$$

For the slag bath:

$$\rho_2 C_{2\varepsilon}(T_{2\varepsilon}) \frac{\partial T_{2\varepsilon}}{\partial t} = \frac{\partial}{\partial x}\left(k_{2\varepsilon}(T_{2\varepsilon}) \frac{\partial T_{2\varepsilon}}{\partial x}\right) - (AT_{2\varepsilon} - B)\frac{\partial F_{\varepsilon}(T_{2\varepsilon})}{\partial t}; \quad d < x < D \text{ and } 0 < t \leqslant t_{\mathrm{f}} \tag{7d}$$

$$k_{2\varepsilon}(T_{2\varepsilon}) \frac{\partial T_{2\varepsilon}}{\partial x} = q''(t) + \varepsilon\Delta q''(t); \quad x = D \text{ and } 0 < t \leqslant t_{\mathrm{f}} \tag{7e}$$

$$T_{2\varepsilon} = T_{02}; \quad d < x < D \text{ and } t = 0 \tag{7f}$$

At the wall/slag interface:

$$k_1 \frac{\partial T_{1\varepsilon}}{\partial x} = k_{2\varepsilon}(T_{2\varepsilon}) \frac{\partial T_{2\varepsilon}}{\partial x}; \quad x = d \text{ and } 0 < t \leqslant t_{\mathrm{f}} \tag{7g}$$

$$T_{1\varepsilon} = T_{2\varepsilon}; \quad x = d \text{ and } 0 < t \leqslant t_{\mathrm{f}} \tag{7h}$$

where $A = \rho_2(C_{2l} - C_{2s})$ and $B = A\ T_{\mathrm{ref}} - \rho_2 L$.

Finally, the sensitivity problem is calculated by applying the following limiting process:

$$\lim_{\varepsilon \to 0} \frac{D_{\varepsilon}(T_{\varepsilon}) - D(T)}{\varepsilon} = 0 \tag{8}$$

$D(T)$ and $D_{\varepsilon}(T_{\varepsilon})$ stand for the equations of the original direct problem (Eqs. (1)) (without perturbations) and for the equations of the perturbed direct problem (Eqs. (7)), respectively. The resulting sensitivity functions $\Delta T_1(x, t)$ and $\Delta T_2(x, t)$ are then formulated as

For the brick wall:

$$\rho_1 C_1 \frac{\partial \Delta T_1}{\partial t} = k_1 \frac{\partial^2 \Delta T_1}{\partial x^2}; \quad 0 < x < d \text{ and } 0 < t \leqslant t_{\mathrm{f}} \tag{9a}$$

$$k_1 \frac{\partial \Delta T_1}{\partial x} = h\Delta T_1; \quad x = 0 \text{ and } 0 < t \leqslant t_{\mathrm{f}} \tag{9b}$$

$$\Delta T_1 = 0; \quad 0 < x < d \text{ and } t = 0 \tag{9c}$$

For the slag bath:

$$\rho_2 \frac{\partial [C_2(T_2)\Delta T_2]}{\partial t} = \frac{\partial^2 [k_2(T_2)\Delta T_2]}{\partial x^2} - AT_2 \frac{\partial(\Delta T_2 F'(T_2))}{\partial t} - A\Delta T_2 \frac{\partial F(T_2)}{\partial t} + B\frac{\partial(F'(T_2)\Delta T_2)}{\partial t}; \quad d < x < D \text{ and } 0 < t \leqslant t_{\mathrm{f}} \tag{9d}$$

$$\frac{\partial [k_2(T_2)\Delta T_2]}{\partial x} = \Delta q''(t); \quad x = D \text{ and } 0 < t \leqslant t_{\mathrm{f}} \tag{9e}$$

$$\Delta T_2 = 0; \quad d < x < D \text{ and } t = 0 \tag{9f}$$

At the wall/slag interface:

$$k_1 \frac{\partial \Delta T_1}{\partial x} = \frac{\partial [k_2(T_2)\Delta T_2]}{\partial x}; \quad x = d \text{ and } 0 < t \leqslant t_{\mathrm{f}} \tag{9g}$$

$$\Delta T_1 = \Delta T_2; \quad x = d \text{ and } 0 < t \leqslant t_{\mathrm{f}} \tag{9h}$$

where F' is the first derivative of the function F with respect to the temperature T_2.

An expression for the search step size β^k is obtained by minimizing the functional provided in Eq. (4) with respect to β^k at each iteration k, that is

$$\min_{\beta^k} S[q''^{k+1}(t)] = \min_{\beta^k} \int_0^{t_{\mathrm{f}}} [T_{\mathrm{m}}(t) - T_1(x_{\mathrm{m}}, t; q''^k(t) - \beta^k d^k(t))]^2 \mathrm{d}t \tag{10a}$$

By linearizing the term $T_1(x_{\mathrm{m}}, t; q''^k(t) - \beta^k d^k(t))$ and making $d^k(t) = \Delta q''^k(t)$, we obtain

$$T_1(x_{\mathrm{m}}, t; q''^k(t) - \beta^k d^k(t)) \approx T_1(x_{\mathrm{m}}, t; q''^k(t)) - \beta^k \frac{\partial T_1}{\partial q''^k(t)} \Delta q''^k(t) \tag{10b}$$

Let $\Delta T_1(x_{\mathrm{m}}, t; d^k(t)) = \frac{\partial T_1}{\partial q''^k(t)} \Delta q''^k(t)$, and then Eq. (10b) can be written as

$$T_1(x_{\mathrm{m}}, t; q''^k(t) - \beta^k d^k(t)) \approx T_1(x_{\mathrm{m}}, t; q''^k(t)) - \beta^k \Delta T_1(x_{\mathrm{m}}, t; d^k(t)) \tag{10c}$$

$\Delta T_1(x_{\mathrm{m}}, t; d^k(t))$ is the solution of the sensitivity problem at the sensor position x_{m}, obtained from Eqs. (9) by setting $\Delta q''^k(t) = d^k(t)$.

Substituting of Eq. (10c) into Eq. (10a) yields

$$\min_{\beta^k} S[q''^{k+1}(t)] = \min_{\beta^k} \int_0^{t_{\mathrm{f}}} [T_{\mathrm{m}}(t) - T_1(x_{\mathrm{m}}, t; q''^k(t)) + \beta^k \Delta T_1(x_{\mathrm{m}}, t; d^k(t))]^2 \mathrm{d}t \tag{10d}$$

By performing the minimization above, the following search step size is obtained:

$$\beta^k = \frac{\int_0^{t_{\mathrm{f}}} [T_1(x_{\mathrm{m}}, t; q''^k(t)) - T_{\mathrm{m}}(t)]\Delta T_1(x_{\mathrm{m}}, t; d^k(t))\mathrm{d}t}{\int_0^{t_{\mathrm{f}}} [\Delta T_1(x_{\mathrm{m}}, t; d^k(t))]^2 \mathrm{d}t} \tag{10e}$$

7. The adjoint problem and the gradient equation

To derive the adjoint problem, both differential equations (1a) and (1d) of the direct problem are multiplied by the Lagrange multipliers $\lambda_1(x, t)$ and $\lambda_2(x, t)$, respectively. Integrating the resulting expressions over time and in the corresponding space domains and adding the resulting equation to the functional given by Eq. (4), one obtains the following extended functional:

$$S[q''(t)] = \int_0^{t_f} [T_m(t) - T_1(x_m, t; q''(t))]^2 dt + \int_{t=0}^{t_f}\int_{x=0}^{d} \lambda_1(x,t)\left[k_1\frac{\partial^2 T_1}{\partial x^2} - \rho_1 C_1\frac{\partial T_1}{\partial t}\right]dx\,dt + \int_{t=0}^{t_f}\int_{x=d}^{D} \lambda_2(x,t)\left[\frac{\partial}{\partial x}\left(k_2(T_2)\frac{\partial T_2}{\partial x}\right) - \delta H\frac{\partial f}{\partial t} - \rho_2 C_2(T_2)\frac{\partial T_2}{\partial t}\right]dx\,dt \quad (11)$$

It is assumed here that the extended functional given by Eq. (11) is perturbed by an amount $\varepsilon\Delta S[q''(t)]$ when the heat flux $q''(t)$ is perturbed by an amount $\varepsilon\Delta q''(t)$. The variation of the extended functional is then obtained by applying the limiting process

$$\Delta S[q''(t)] = \lim_{\varepsilon\to 0}\frac{S[q''(t)+\varepsilon\Delta q''(t)] - S[q''(t)]}{\varepsilon} \quad (12)$$

which yields

$$\Delta S[q''(t)] = 2\int_{t=0}^{t_f}\int_{x=0}^{d}[T_1 - T_m(t)]\delta(x-x_m)\Delta T_1\,dx\,dt + \int_{t=0}^{t_f}\int_{x=0}^{d}\lambda_1(x,t)\left[k_1\frac{\partial^2\Delta T_1}{\partial x^2} - \rho_1 C_1\frac{\partial \Delta T_1}{\partial t}\right]dx\,dt + \int_{t=0}^{t_f}\int_{x=d}^{D}\lambda_2(x,t)\left[\frac{\partial^2[k_2(T_2)\Delta T_2]}{\partial x^2} - A T_2\frac{\partial(\Delta T_2 F'(T_2))}{\partial t} - A\Delta T_2\frac{\partial F(T_2)}{\partial t} + B\frac{\partial(F'(T_2)\Delta T_2)}{\partial t} - \rho_2\frac{\partial[C_2(T_2)\Delta T_2]}{\partial t}\right]dx\,dt \quad (13a)$$

Integrating the last two terms on the right-hand side of the above equation and using the boundary and initial conditions for the sensitivity problem (Eqs. (9)), we obtain

$$\Delta S[q''(t)] = \int_{t=0}^{t_f}\int_{x=0}^{d}\left[\rho_1 C_1\frac{\partial\lambda_1}{\partial t} + k_1\frac{\partial^2\lambda_1}{\partial x^2} + 2[T_1 - T_m(t)]\delta(x-x_m)\right]\Delta T_1\,dx\,dt + \int_{t=0}^{t_f}\int_{x=d}^{D}\left[\rho_2 C_2(T_2)\frac{\partial\lambda_2}{\partial t} + k_2(T_2)\frac{\partial^2\lambda_2}{\partial x^2} - A\lambda_2\frac{\partial F(T_2)}{\partial t} - B\frac{\partial\lambda_2}{\partial t}F'(T_2) + A\frac{\partial(\lambda_2 T_2)}{\partial t}F'(T_2)\right]\times\Delta T_2\,dx\,dt + \int_{t=0}^{t_f}\left[k_2(T_2)\frac{\partial\lambda_2}{\partial x}\bigg|_{x=d} - k_1\frac{\partial\lambda_1}{\partial x}\bigg|_{x=d}\right]\times\Delta T_1(d,t)\,dt + \int_{t=0}^{t_f}k_1\frac{\partial\Delta T_1}{\partial x}\bigg|_{x=d}[\lambda_1(d,t) - \lambda_2(d,t)]dt + \int_{t=0}^{t_f}\left[k_1\frac{\partial\lambda_1}{\partial x}\bigg|_{x=0} - h\lambda_1(0,t)\right]\Delta T_1(0,t)\,dt - \int_{t=0}^{t_f}k_2(T_2)\frac{\partial\lambda_2}{\partial x}\bigg|_{x=D}\Delta T_2(D,t)\,dt - \int_{x=0}^{d}\rho_1 C_1\lambda_1(x,t_f)\Delta T_1(x,t_f)\,dx + \int_{x=d}^{D}B\lambda_2(x,t_f)F\prime(T_2(x,t_f))\Delta T_2(x,t_f)\,dx - \int_{x=d}^{D}\rho_2 C_2(T_2(x,t_f))\lambda_2(x,t_f)\Delta T_2(x,t_f)\,dx - \int_{x=d}^{D}A\lambda_2(x,t_f)T_2(x,t_f)\Delta T_2(x,t_f)F'(T_2(x,t_f))\,dx + \int_{t=0}^{t_f}\lambda_2(D,t)\Delta q''(t)\,dt \quad (13b)$$

The boundary value problem for the Lagrange multipliers $\lambda_1(x, t)$ and $\lambda_2(x, t)$ is obtained by allowing the first ten integral terms on the right-hand side of Eq. (13b) to vanish. This leads to the following adjoint problem:

For the brick wall:

$$\rho_1 C_1\frac{\partial\lambda_1}{\partial t} + k_1\frac{\partial^2\lambda_1}{\partial x^2} + 2[T_1 - T_m(t)]\delta(x-x_m) = 0; \quad 0 < x < d \text{ and } 0 < t < t_f \quad (14a)$$

$$k_1\frac{\partial\lambda_1}{\partial x} = h\lambda_1; \quad x = 0 \text{ and } 0 < t < t_f \quad (14b)$$

$$\lambda_1 = 0; \quad 0 < x < d \text{ and } t = t_f \quad (14c)$$

For the slag bath:

$$\rho_2 C_2(T_2)\frac{\partial\lambda_2}{\partial t} + k_2(T_2)\frac{\partial^2\lambda_2}{\partial x^2} - A\lambda_2\frac{\partial F(T_2)}{\partial t} - B\frac{\partial\lambda_2}{\partial t}F'(T_2) + A\frac{\partial(\lambda_2 T_2)}{\partial t}F'(T_2) = 0; \quad d < x < D \text{ and } 0 < t < t_f \quad (14d)$$

$$\frac{\partial\lambda_2}{\partial x} = 0; \quad x = D \text{ and } 0 < t < t_f \quad (14e)$$

$$\lambda_2 = 0; \quad d < x < D \text{ and } t = t_f \quad (14f)$$

At the wall/slag interface:

$$k_1\frac{\partial\lambda_1}{\partial x} = k_2(T_2)\frac{\partial\lambda_2}{\partial x}; \quad x = d \text{ and } 0 < t < t_f \quad (14g)$$

$$\lambda_1 = \lambda_2; \quad x = d \text{ and } 0 < t < t_f \quad (14h)$$

Finally, in the limiting process given by (12), the following integral term is left:

$$\Delta S[q''(t)] = \int_0^{t_f}\Delta q''(t)\lambda_2(D,t)\,dt \quad (15a)$$

From the assumption that $q''(t) \in L_2(0,t_f)$, one can write:

$$\Delta S[q''(t)] = \int_0^{t_f}\Delta q''(t)\nabla S[q''(t)]\,dt \quad (15b)$$

Comparison of Eqs. (15a) and (15b) yields the gradient equation for the functional:

$$\nabla S[q''(t)] = \lambda_2(D,t) \quad (16)$$

8. Stopping criterion

In the absence of noise, the iterative process, Eq. (5a), is repeated until the functional $S[q''(t)]$ satisfies the following stopping criteria:

$$S[q''^{k+1}(t)] - S[q''^{k}(t)] < \zeta_1 \tag{17a}$$

where ζ_1 is of the order of 10^{-4}.

In the presence of noise, the discrepancy principal [14] given by Eq. (17b) is used to stopping the iterative procedure.

$$S[q''^{k+1}(t)] < \zeta_2 \tag{17b}$$

where $\zeta_2 = \sigma^2 t_f$, σ is the standard deviation of measurement errors.

In this case, if the functional $S[q''(t)]$ has a minimum value that is larger than ζ_2, the criterion given by (17a) is used.

9. Computational algorithm

The main steps for the solution of the inverse problem via the conjugate gradient method with the adjoint equation may be summarized as follows:

First, the iteration number k is set to zero and an initial value for the unknown heat flux $q''^0(t)$ is made.

Step 1: The direct problem (set of Eqs. (1)) is solved for the temperatures $T_1(x, t)$ and $T_2(x, t)$ at a new time step;
Step 2: If convergence is satisfied (Eq. (17a) or (17b)), stop. Otherwise, go to 3;
Step 3: The adjoint problem (set of Eqs. (14)) is solved for the Lagrange multipliers $\lambda_1(x, t)$ and $\lambda_2(x, t)$;
Step 4: The gradient of the functional $\nabla S[q''(t)]$ is obtained from Eq. (16);
Step 5: The conjugation coefficient γ^k is estimated from Eq. (5c) and the direction of descent $d^k(t)$ is calculated from Eq. (5b);
Step 6: The sensitivity problem, Eqs. (9), is solved for $\Delta T_1(x, t)$ and $\Delta T_2(x, t)$, by setting $\Delta q''(t) = d^k(t)$;
Step 7: The search step size β^k is computed from Eq. (10e);
Step 8: The new estimate $q''^{k+1}(t)$ is obtained from Eq. (5a); Return to step 1.

Once the inverse solution $q''_{\text{estimated}}(t)$ of the unknown heat flux $q''(t)$ is achieved, the bank thickness $E_b(t)$ is easily predicted with a direct enthalpy method using the estimation $q''_{\text{estimated}}(t)$.

10. Results and discussion

The above inverse heat transfer method was thoroughly tested for estimating the unknown heat flux $q''(t)$, and therefore, for predicting the bank thickness $E_b(t)$. Numerical simulations were carried out using typical operating conditions that prevail inside industrial smelting furnaces. The brick wall is 0.7 m thick and the studied slag layer is 0.5 m wide (Fig. 2). The physical properties of the refractory bricks and of the slag are summarized in Table 1. For the left boundary condition, the surrounding temperature is kept constant, $T_\infty = 300$ K, and the average heat transfer coefficient is set equal to $h = 15$ W/(m^2 K). At time $t = 0$, the initial temperature is assumed to be: $T_0(x) = (x/D)(900 - T_\infty) + T_\infty$ pour $0 \leqslant x \leqslant D$.

The 'measured temperatures' $T_m(t)$ were obtained from the solution $T_1(x_m, t)$ of the direct conduction-dominated phase change problem at the sensor location x_m, by using the following prescribed time variation for the heat flux $q''(t)$:

$$q''(t) = \begin{cases} 2.4\times10^4 + 0.24\times10^4 \sin(2\pi t/86400); & 0 \leqslant t \leqslant 86400 \\ 0.0; & 86400 < t \leqslant 172800 \\ 2.4\times10^4 + 0.24\times10^4 \sin(2\pi t/86400); & 172800 < t \leqslant 259200 \\ 0.0; & 259200 < t \leqslant 345600 \end{cases} \tag{18}$$

The solution for the direct problem subject to the above time varying heat flux yields, during the four day period, a bank that reaches three times its maximum thickness of 0.5 m, i.e. the slag layer is completely solidified, and a bank that passes two times through minimum values. The 'measured temperatures' are then estimated by taking into account random noise:

$$T_m(t) = T_1(x_m, t) + \omega\sigma \tag{19}$$

σdetermines the noise level, which may take the value of 0.0 (no measurement error), $2\%T_{max}$ and $4\%T_{max}$, T_{max} being the maximum measured temperature at x_m. ω is a random number in the range $-2.576 \leqslant \omega \leqslant 2.576$. σ is the standard deviation of the measurement errors which are assumed to be the same for all experimental data, and ω is the Gaussian distributed random error. The above range for the ω values corresponds to 99% confidence bound for the temperature measurement.

All simulations presented here were conducted with a grid size of 70 uniformly distributed control volumes inside the brick wall and 50 control volumes distributed in the

Table 1
Thermo physical properties of the materials

Brick	
ρ_1	2851 kg/m^3
C_1	1000 J/(kg K)
k_1	8 W/(m K)
Slag	
ρ_2	3400 kg/m^3
$C_{2s} = C_{2l}$	1026 J/(kg K)
k_{2s}	4 W/(m K)
k_{2l}	877 W/(m K)
L	823000 J/kg
T_s	1730 K
T_l	1890 K
T_{ref}	1973 K

slag layer. Calculations performed with finer meshes did not improve perceptibly the numerical predictions. For the inverse analysis, calculations are launched with an initial value of $q''^0(t) = 0.0$. This means that the initial estimation of the bank thickness is $E_b^0(t) = 0.5$.

To further check the accuracy of the inverse method, two different estimation errors are defined:

$$e_1 = \frac{\|q''_{\text{estimated}} - q''_{\text{exact}}\|^2_{L_2}}{\|q''_{\text{exact}}\|^2_{L_2}} \times 100 \tag{20}$$

which is the estimation error on the predicted heat flux $q''(t)$ and

$$e_2 = \frac{\|E_{\text{b,estimated}} - E_{\text{b,exact}}\|^2_{L_2}}{\|E_{\text{b,exact}}\|^2_{L_2}} \times 100 \tag{21}$$

which is the estimation error on the predicted bank thickness $E_b(t)$. $\|\cdot\|^2_{L_2}$ is the L_2-norm and the subscripts *estimated* and *exact* refer to the estimated and the exact functions, respectively.

As an example, Figs. 3 and 4 show the effect of the thermocouple position (one is embedded in the brick wall at a depth of $x_m = 0.01$ m and the other at $x_m = 0.69$ m) on the predicted heat flux and bank thickness, respectively. Examination of Fig. 3 reveals that the accuracy of the predicted heat flux is improved as the distance separating the thermocouple from the right boundary condition is reduced. On the other hand, the effect of this distance on the predicted bank thickness is nearly imperceptible (Fig. 4). In both cases, the predictions are excellent. From an industrial point of view, this finding has important implications: one can embed the thermocouple at a depth of only one centimetre inside the brick wall and it will provide reasonably accurate estimates of the bank thickness without affecting the structural integrity of the wall itself.

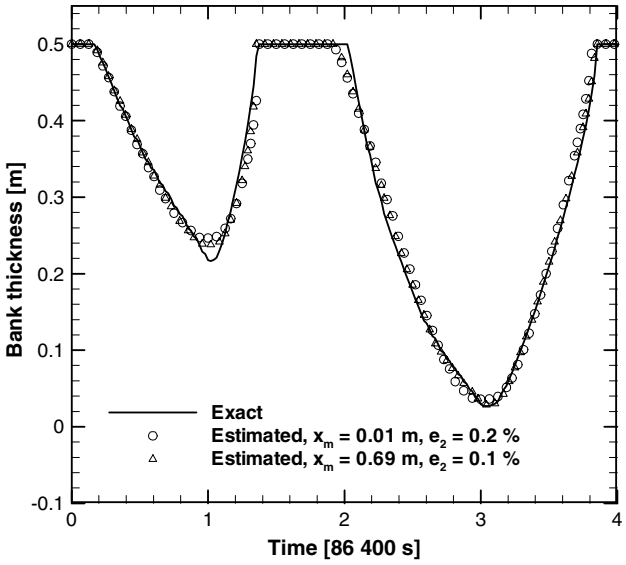

Fig. 4. Effect of x_m on the predicted bank thickness $E_b(t)$ with $\sigma = 0.0$.

The effect of the noise level σ on the predicted bank thickness $E_b(t)$ is illustrated in Fig. 5. T_{max} is the maximum temperature measured at the location $x_m = 0.10$ m. These results were obtained with a time step of 900 s for the case $\sigma = 2\%T_{max}$ and a time step of 450 s for the case $\sigma = 4\%T_{max}$. It is seen that the predictions for the bank thickness remain accurate even for noise levels as large as $\sigma = 4\%T_{max}$.The effect of the thermal contact resistance between the refractory brick wall and the slag bank R''_{cont} was also investigated. R''_{cont} is a complex function of the slag composition, which in turn depends on the operating conditions. It is also a function of the brick type and slag infiltration into the gaps between the bricks. This resistance may be taken into account in the model by modifying Eqs. (1g) and (1h) to

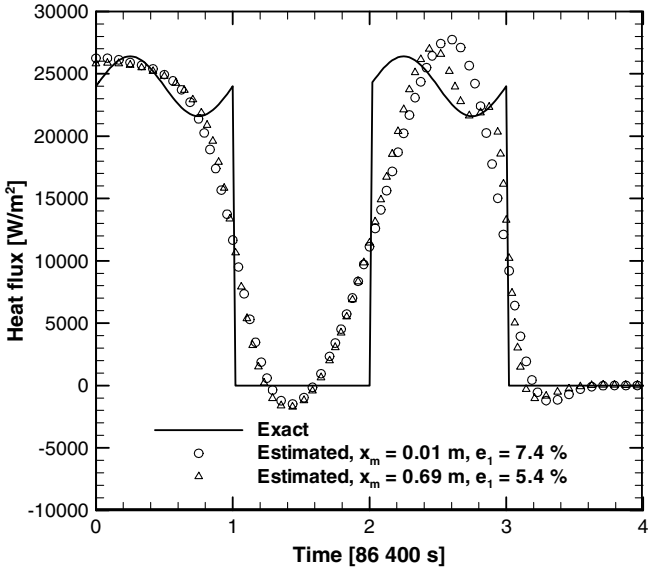

Fig. 3. Effect of x_m on the predicted heat flux $q''(t)$ with $\sigma = 0.0$.

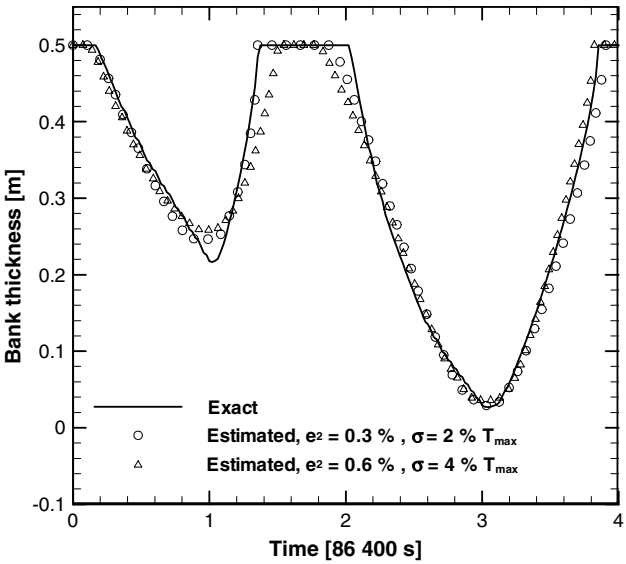

Fig. 5. Effect of σ on the predicted bank thickness $E_b(t)$ for $x_m = 0.01$ m.

$$k_1 \frac{\partial T_1}{\partial x} = (R''_{\text{cont}})^{-1}(T_2 - T_1) = k_2(T_2)\frac{\partial T_2}{\partial x}; \quad x = d \text{ and } 0 < t \leqslant t_f \tag{22}$$

by changing Eqs. (9g) and (9h) to

$$k_1 \frac{\partial \Delta T_1}{\partial x} = (R''_{\text{cont}})^{-1}(\Delta T_2 - \Delta T_1) = \frac{\partial [k_2(T_2)\Delta T_2]}{\partial x}; \quad x = d \text{ and } 0 < t \leqslant t_f \tag{23}$$

and by replacing Eqs. (14g) and (14h) by

$$k_1 \frac{\partial \lambda_1}{\partial x} = (R''_{\text{cont}})^{-1}(\lambda_2 - \lambda_1) = k_2 \frac{\partial \lambda_2}{\partial x}; \quad x = d \text{ and } 0 < t \leqslant t_f \tag{24}$$

Simulations were carried out to examine the effect of R''_{cont} on the predicted bank thickness. Typical values ranging from $5 \times 10^{-3}\ \text{m}^2\,\text{K/W}$ to $5 \times 10^{-2}\ \text{m}^2\,\text{K/W}$ were investigated. As expected, the predictions deteriorate as the magnitude of this resistance increases. Accurate results may however be obtained simply by embedding the thermocouple deeper inside the brick wall.

The final example illustrates how the above inverse heat transfer model may be employed, during the operation of a smelting furnace, to prevent the loss of the protective bank. In the present case, the bank is not allowed to shrink to a thickness smaller than say 0.1 m. The heat flux is provided by Eq. (18). The corresponding bank thickness predicted by the inverse method with $x_m = 0.01$ m, $\sigma = 1\% T_{\max}$ and $t_f = 207\,000$ s is depicted in Fig. 6. This figure reveals that at time $t = t_f = 207\,000$ s, the bank is 0.19 m thick and its melting rate is $\bar{v} = \frac{\overline{ds}}{dt} \approx -7.4 \times 10^{-6}$ m/s. At this rate, it is then expected that the bank will reach a minimum thickness of 0.1 m at time $t = 218684$ s. By feeding this information to the operating system, the scenario for the heat flux (Eq. (18)) is then corrected in advance and the loss of the bank is avoided (Fig. 7).

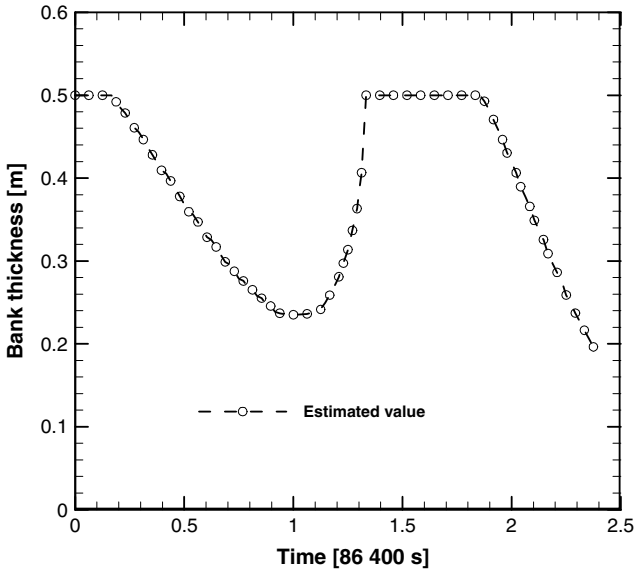

Fig. 6. Predicted bank thickness for $x_m = 0.01$ m, $\sigma = 1\% T_{\max}$.

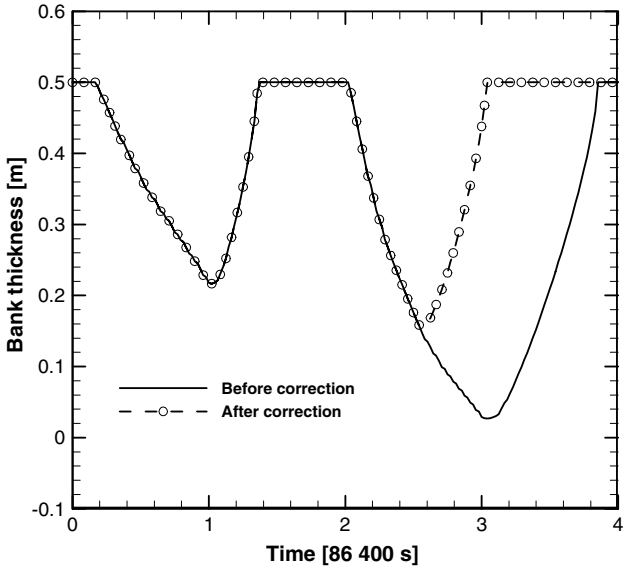

Fig. 7. Predicted bank thickness with and without corrected heat flux.

11. Conclusion

An inverse phase change heat transfer method has been developed for predicting the time evolution of banks covering the surface of refractory brick walls inside high temperature smelting furnaces. The numerical model rests on the conjugate gradient solution method with the adjoint equation. It predicts banks thickness and motion relying on the thermal conditions prevailing outside the furnace and temperature measurements taken at one location inside the brick wall. Simulations were carried out to examine the effect of different parameters on the predictive capabilities of the method. Results have revealed that the method remains accurate in spite of the fact that the temperature measurements inside the wall are noisy and are taken at a depth of only one centimetre. An example showing how the present inverse method can be used to warn on the imminent loss of the protective bank during the operation of a smelting furnace was provided.

Acknowledgement

The authors are very grateful to the Natural Sciences and Engineering Research Council of Canada and to the 'Ministère des Ressources naturelles du Québec' for their financial support.

References

[1] M. Orfeuil, Electric Process Heating, Battelle Press, 1987.
[2] J. Szekely, J. McKelliget, M. Choudhary, Heat-transfer fluid flow and bath circulation in electric-arc furnaces and DC plasma furnaces, Ironmaking Steelmaking 10 (4) (1983) 169–179.
[3] Y.Y. Sheng, G.A. Irons, D.G. Tisdale, Transport phenomena in electric smelting of nickel matte: Part I. Electric potential distribution, Metall. Mater. Trans. B 29B (1998) 77–83.

[4] J. Alexis, M. Ramirez, G. Trapaga, P. Jönsson, Modeling of a DC electric arc furnace—Heat transfer from the arc, ISIJ Int. J. 40 (11) (2000) 1089–1097.
[5] V.R. Voller, C.R. Swaminathan, General source-based method for solidification phase change, Numer. Heat Transfer 19 (1991) 175–189.
[6] N. Zabaras, S. Mukherjee, O. Richmond, An analysis of inverse heat transfer problems with phase changes using an integral method, J. Heat Transfer 110 (1988) 554–561.
[7] N. Zabaras, Y. Ruan, A deforming finite element method analysis of inverse Stefan problems, Int. J. Numer. Methods Engrg. 28 (1989) 295–313.
[8] Y. Ruan, N. Zabaras, An inverse finite element technique to determine the change of phase interface location in two-dimensional melting problems, Commun. Appl. Numer. Methods 7 (1991) 325–338.
[9] M.A. Katz, B. Rubinsky, An inverse finite element technique to determine the change of phase interface location in one-dimensional melting problems, Numer. Heat Transfer 7 (1984) 269–283.
[10] D. Frederick, R. Greif, A method for the solution of heat transfer problems with a change of phase, J. Heat Transfer ASME 107 (1985) 520–526.
[11] Y.F. Hsu, B. Rubinsky, K. Mahin, An inverse finite element method for the analysis of stationary arc welding processes, J. Heat Transfer 108 (1986) 734–741.
[12] M. Samai, Y. Jarny, D. Delaunay, An optimization method using an adjoint equation to identify solidification front location, Numer. Heat Transfer 23 (1993) 67–89.
[13] T. Loulou, E.A. Artyukhin, J.P. Bardon, Estimation of thermal contact resistance during the first stages of metal solidification process: I—Experiment principle and modelisation, Int. J. Heat Mass Transfer 42 (1999) 2119–2127.
[14] M.N. Ozisik, H.R.B. Orlande, Inverse Heat Transfer: Fundamentals and Applications, Taylor and Francis, New York, 2000.
[15] T. Ma, J.D. Lavers, A finite element iterative simulation of coupled electrothermal effects in an electric smelting furnace, IEEE Trans. Mag. MAG-21 (1985) 2416–2419.